CMOS Micromechanical Bandpass Filter Design Using a Hierarchical MEMS Circuit Library

Qi Jing†, Hao Luo†, Tamal Mukherjee†, L. Richard Carley†, and Gary K. Fedder†*
†Department of Electrical and Computer Engineering and *The Robotics Institute
Carnegie Mellon University, Pittsburgh, PA 15213-3890 USA

ABSTRACT

A 550 kHz CMOS micromechanical bandpass filter, is designed using a parameterized cell library, "NODAS," for schematic representation and behavioral HDL simulation. The filter employs a unique resonator and coupling spring structure implemented in a CMOS-MEMS technology. As an alternative design method, an equivalent SPICE model is derived for the filter. Frequency response around the filter passband from SPICE simulation matches that from NODAS simulation to within 2%. Compared to an equivalent SPICE model methodology, the NODAS methodology enables convenient composition and simulation of complicated MEMS. The experimental result of the fabricated device shows that the center frequency and bandwidth match NODAS simulation to within 3%, which provides component level validation of the NODAS-based MEMS design methodology. Nonideal effects such as manufacturing variations are also simulated and discussed.

INTRODUCTION

Bandpass filters are key components of transceivers in communication technology. Conventional physical implementations of bandpass filters are based on mechanical devices such as crystal resonators, or electronic devices such as transistor LC circuits. Mechanical resonators have high quality factors, but can only be interfaced with electronics at the board level, limiting miniaturization and transceiver performance. Electrical devices can be integrated, however, the performance of electronic filters is restricted by the limited quality factor of the electronics.

IC-compatible surface micromachining fabrication technology provides a potential solution to this problem. High-Q mechanical resonators can be implemented on-chip [1] [2] and integrated with electronic interface circuits, forming miniaturized, high-performance Microelectromechanical Systems (MEMS). To date, micromechanical bandpass filters, with center frequencies ranging from 300 kHz to 35 MHz, have been successfully implemented using a polysilicon IC-compatible surface micromachining fabrication technique [3].

In this paper, the devices are fabricated in a CMOS-MEMS technology in which microstructures are obtained by post-process release following conventional CMOS IC fabrication [4]. Figure 1 shows the main steps of this process. In this process, the microstructures are fabricated simultaneously with the electronics. The metal-3 layer has three roles: as the structural mask during release, as a protection mask for electrical circuits outside of mechanical structures, and as the electrical wiring on top of the mechanical structures. The conservative design rule spacing between mechanical and electrical parts is about 30 μm, which is less than other IC-compatible surface micromachining processes. Moreover, this CMOS-MEMS process allows microstructures consisting of multiple conductive layers, enabling more flexible electrical connectivity. To take advantage of this characteristic, differential electrostatic comb drives are employed in the presented bandpass filter design. Compared to conventional single-finger interdigited comb drives, differential comb drives have higher sensitivity in capacitance change. Therefore, they are more efficient in electrostatic driving and sensing.

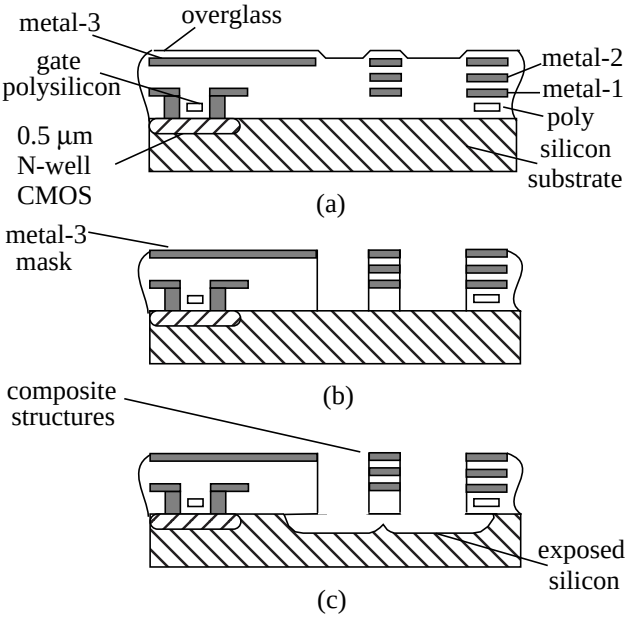

Figure 1: CMOS-MEMS process (a) CMOS chip after fabrication (b) anisotropic RIE removes dielectric (c) isotropic RIE undercuts silicon substrate

The micromechanical bandpass filters are systems composed of multiple resonators, coupling networks, and electrical interface circuits. They involve physical interactions between mechanical and electrostatic domains. Appropriate MEMS CAD tools are needed to handle the design and multi-domain simulation of such complicated systems.

Mature FEM simulators, such as ABAQUS™, are good for mechanical design, but do not support simulation in the electrical domain. Novel CAD tools such as MEM-

CAD™ can handle electrostatic simulations, but do not consider electrical circuits simultaneously with electrostatic simulation. Equivalent SPICE models based on circuit analogies of mechanical devices have previously been used for co-simulation of mechanical device and electronics for the filter system [1]. However, since variables, devices and effects in mechanical domain are not represented in their native natures, the constitution of equivalent SPICE models inevitably involves approximations and much effort.

In this paper, we present a design methodology for micromechanical bandpass filters based on behavioral models of mechanical elements, which uses the inherent advantage of behavioral models in multi-domain modeling and simulation.

The tool we used is NODAS (Nodal Design of Actuators and Sensors). It is a hierarchical cell library for behavioral modeling and nodal simulation of MEMS [5]. The NODAS cell library consists of symbols and models of elements commonly found in suspended MEMS design, such as anchors, beams, plates and electrostatic comb drives. These symbols can be wired together to quickly compose a MEMS schematic. Lower level components (e.g., a resonators) can serve as building-blocks for higher level schematics of more complicated systems, like filters. Each element in NODAS has a parameterized behavioral model, written in the Verilog-A Analog Hardware Description Language [6]. In this paper, simulation of the entire filter system is done using Cadence's Spectre™, in which co-simulation of electrical circuits is supported.

Figure 2 shows a simple cantilever beam as an example of a NODAS schematic [5]. NODAS behavioral models are lumped parameter models. The behavior of the beam is lumped at its two ends. At each end, there are two groups of nodes: δx, δy, $\delta\theta$ are translational and rotational nodes, and v is the electrical node. For electrical nodes, voltages are across variables, and currents are through variables. For mechanical nodes, translational and rotational displacements are across variables, forces and torques are through variables. The beam model is geometrically parameterized to allow the user to specify size and orientation of each beam instance. A set of technology constants associates the models to a specific fabrication process. By connecting the beam to an anchor element, which specifies the attachment to the substrate, the schematic for a cantilever beam can be easily composed.

In this paper, we first present the topology of the filter in section 2. Then an equivalent SPICE model of the filter is developed in section 3, followed by a comparison of frequency responses from SPICE simulation and NODAS simulation. Simulation of nonideal effects such as manufacturing variations are further discussed in section 4. Section 5 presents the experimental result of the filter, with comparison to the NODAS simulation result.

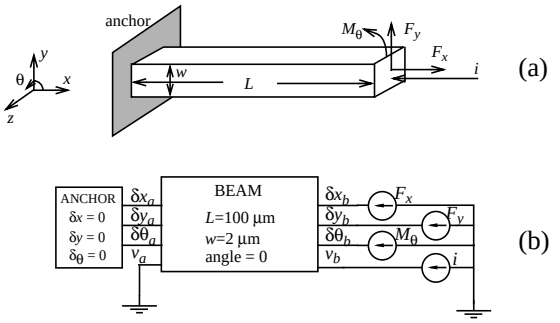

Figure 2: An example of NODAS cells, (a) a cantilever beam (b) the NODAS schematic of cantilever beam.

FILTER TOPOLOGY

The maximum resonant frequency achievable by micromechanical resonators is limited by many factors. For example, the effective finite mass of mechanical springs limits the maximum resonant frequency, and the minimum gap between fingers due to process design rules limits efficient electrostatic actuation of stiff microstructures. Thus, the application feasibility of micro-resonators in RF regions is still being studied. However, since microresonators working at 10 kHz to 1MHz are very stable and reliable, the IF region is a suitable application area. Our bandpass filter example is designed to be centered at 550 kHz, which is a typical value for IF applications.

The bandpass filter presented is composed of three identical resonators, each resonating at 550 kHz, coupled by springs. Figure 3 shows the operating principle of this type of mechanical filter.

According to the analysis of coupled resonators [7], all the adjacent resonators vibrate in phase at the lowest natural frequency, and 180 degrees out of phase at the highest natural frequency. Resonances between the lowest and the highest natural frequencies have displacement patterns where a resonator may be in phase, out of phase, or stationary with respect to its neighbor. The filter in this paper has three resonant modes, as shown in Figure 3(a). The three resonant peaks scatter around the resonant frequency of a single resonator, forming a passband shown in Figure 3(b). The location and spacing of the three peaks are determined by the stiffness of the coupling springs. Therefore, the coupling springs can be designed to obtain the desired center frequency and bandwidth.

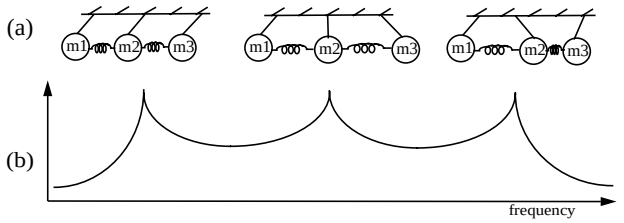

Figure 3: Three resonance modes(a) and peaks(b) of the mechanical filter system

The topology of the filter presented in this paper is shown in Figure 4, which is the schematic of the filter created in Cadence™ using NODAS cells. Both mechanical structures and interface circuitry are included.

Each of the three resonators is composed of a center proof mass, crab-leg springs, and differential electrostatic comb drives (for actuating and sensing). Figure 5 shows the electrical connectivity inside the driving resonator. The stator fingers are connected to the input voltage V_{in} with DC bias at 0 V, and the rotor fingers are differentially DC biased at V+ and V-, therefore, the fingers theoretically will have no DC position offset. When a sinusoidal voltage is applied to the stator fingers, electrostatic forces will be generated to actuate the suspended microresonators. In this design, the comb fingers consist of a stack of three metal layers and a polysilicon layer. These layers are electrically connected to the same voltage. This construction maximizes the active sidewall area of capacitance, therefore, the electrostatic forces are maximized.

The coupling spring topology employed in this design is named an "O" spring, as shown in Figure 4. The springs are composed of beams with metal-2 and metal-1 only, in order to obtain softer springs, and therefore, narrower bandwidth. The three resonators resonate in x-direction, and are coupled at the center plates of each resonator.

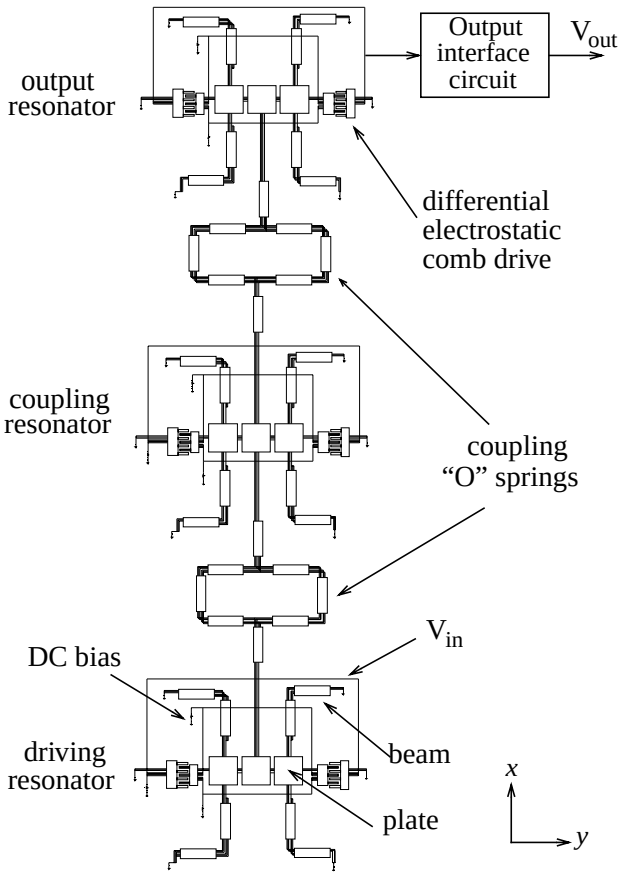

Figure 4: Schematic of the micromechanical bandpass filter in NODAS.

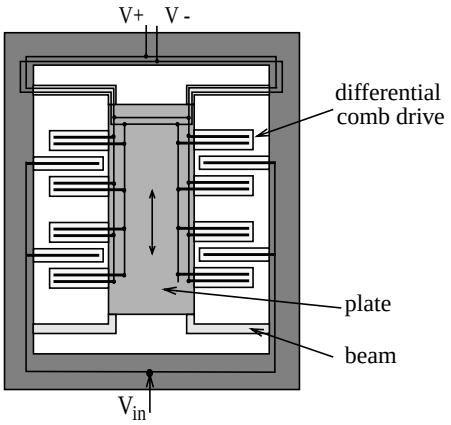

Figure 5: Electrical connectivity of the driving resonator.

EQUIVALENT SPICE MODEL

System level simulations of micromechanical filters was previously done using equivalent SPICE models [1]. To study the use of the equivalent SPICE models as an alternative design methodology, a SPICE model for our filter design is developed.

The circuit analogy of the filter system is based on representing a mechanical resonator as an ideal second-order system, composed of a lumped mass, a spring, and a damper. The series equivalent circuit of the resonator are shown in Figure 6. The analogy relations are given in Table 1.

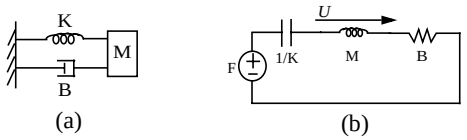

Figure 6: (a) Diagram of a second-order system, (b) Equivalent circuit (in series analogy)

Table 1. Analogy between mechanical and electrical domains

mechanical	**electrical analogy**
force F(s)	voltage V(s) = F(s)
velocity U(s) = s X(s)	current I (s) = U(s)
mass = M	inductor = L = M
spring = K	capacitor = C = 1/K
damper = B	resistor = R = B

Using the resonator as a building block, and assuming the coupling springs are ideal, massless springs with spring constants of K_{12} and K_{23} in the expected resonant modes, we can constitute the mechanical schematic of the filter system as shown in Figure 7(a). The equivalent circuit of the filter in series analogy is shown in Figure 7(b), where the coupling capacitors are analogous to the coupling springs.

The mechanical-electrical analogy can be seen in the transfer functions of the mechanical system (Figure 7(a)) in the frequency domain:

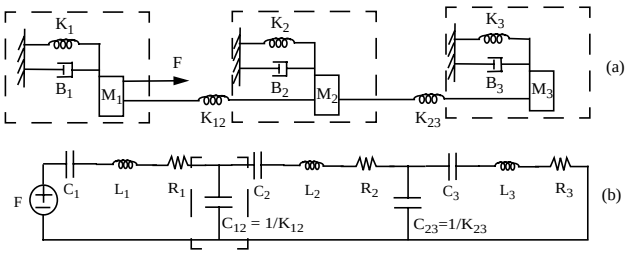

Figure 7: (a) Mechanical schematic of the filter with lumped parameters, (b) Equivalent circuit of the filter with coupling capacitor network.

$$\left[M_1 s^2 + B_1 s + (K_1 + K_{12})\right] X_1(s) - K_{12} X_2(s) = F(s) \quad (1)$$

$$-K_{12} X_1(s) + \left[M_2 s^2 + B_2 s + (K_{12} + K_{23} + K_2)\right] X_2(s) - K_{23} X_3(s) = 0 \quad (2)$$

$$-K_{23} X_2(s) + \left[M_3 s^2 + B_3 s + (K_3 + K_{23})\right] X_3(s) = 0 \quad (3)$$

and the transfer functions of the electrical system (Figure 7(b)) in the frequency domain:

$$\left[L_1 s + R_1 + \left(\frac{1}{sC_1} + \frac{1}{sC_{12}}\right)\right] I_1(s) - \frac{1}{sC_{12}} I_2(s) = V(s) \quad (4)$$

$$-\frac{1}{sC_{12}} I_1(s) + \left[L_2 s + R_2 + \left(\frac{1}{sC_2} + \frac{1}{sC_{12}} + \frac{1}{sC_{23}}\right)\right] I_2(s) - \frac{1}{sC_{23}} I_3(s) = 0 \quad (5)$$

$$-\frac{1}{sC_{23}} I_2(s) + \left[L_3 s + R_3 + \left(\frac{1}{sC_3} + \frac{1}{sC_{23}}\right)\right] I_3(s) = 0 \quad (6)$$

Applying the analogy shown in Table 1 to Eq (4)-(6), and comparing to Eq (1)-(3), we find that the coupling capacitors are:

$$C_{12} = 1/K_{12} \quad , \quad C_{23} = 1/K_{23},$$

The equivalent RLC values are the same as those used in the equivalent series circuit for a single resonator (Figure 6). In our design, the three resonators are identical, and so are the coupling springs. Thus,
$R_1=R_2=R_3=R=B$, $L_1=L_2=L_3=L=M$, $C_1=C_2=C_3=C=1/K$, $C_{12} = C_{23} = C_{ij} = 1/K_{ij}$.

K_{ij} is the effective spring constant of the coupling structure in the expected resonant mode. It is obtained through NODAS simulation in our design. It can also be extracted by finite element analysis.

We see that the SPICE model is a lumped parameter model, as are the NODAS models, but the SPICE model is lumped at the device level, instead of a lower, element, level. Therefore, if the topology of the resonator or the coupling springs are changed, or if the geometric parameters of any component are changed, the effective lumped parameters *M, B, K,* and K_{ij} will need to be rederived. This procedure is cumbersome, especially for little understood topologies. However, in NODAS, since each atomic component (e.g., beam, plate. *etc.*) has a parameterized behavioral model, we can easily change the geometric parameters or the connectivity of element instances to simulate a new structure with updated sizes or even updated topologies without re-analyzing the new structure theoretically.

The equivalent SPICE model shown above doesn't model the comb drives. Effect of simple interdigited comb drives can be linearized and added into the SPICE model [1], but for more complicated cases such as differential comb drives, linearization is not easy to implement. Therefore, when we compare the SPICE simulation to the NODAS simulation, output stage current is chosen as the output variable, which is analogous to the velocity of the output resonator in the mechanical schematic, as shown in Table 1.

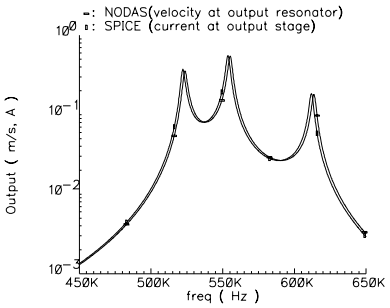

Figure 8: Frequency-domain simulation in NODAS and SPICE, showing bandpass characteristic in air

SIMULATION RESULTS

1. Simulations in NODAS and SPICE

As mentioned above, the equivalent SPICE model represents the mechanical resonators as second-order systems of lumped parameters M, K and B, and represent the coupling beams as massless ideal springs with spring constant K_{ij}. Therefore, when we compare the simulations in NODAS and SPICE, all the beams in NODAS schematic are set to be massless.

Figure 8 shows the frequency response of the filter. We can see that NODAS and SPICE results match closely to within 2%. Theoretically, they should be identically the same. The slight difference is due to numerical error in calculating the effective M, K, B and K_{ij}.

2. Finite-Mass Effect of Beams

In reality, both crab-leg and coupling beams have finite masses, instead of being massless. The finite masses of crab-leg beams will shift the center frequency of the filter and thus affect coupling. The mass of coupling beams will add to the effective mass of adjacent resonators so as to shift resonant frequencies and cause passband distortion. Although the theoretical formula of the effective mass can be derived for the crab-leg springs, such a derivation is cumbersome and may require more effort for other new resonator topologies. Calculating the effective mass of coupling beams requires even more effort.

In NODAS, lumped parameter models are at the layout-based element-level (beams), instead of device-level (resonators). Thus, issues like finite mass of beams is inherently considered. Figure 9 compares NODAS simulation results with and without coupling beam mass. The filter center frequency is decreased by 4% due to the effect of beam mass.

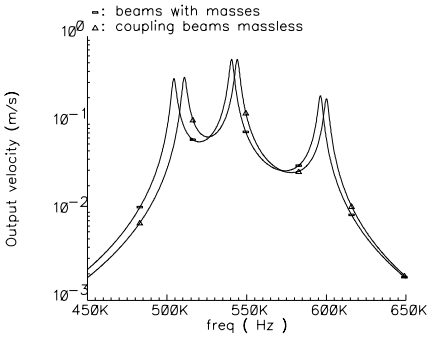

Figure 9: Effect of finite masses of coupling beams

3. Electrical Spring Softening Effect

In the comparison between NODAS and SPICE, the input corresponded to the comb force and the output to the proof mass velocity due to a lack of SPICE comb model. Actually, both the input and output of the filter system are voltages. Figure 10 shows the velocity of the output resonator when input is force, and the velocity and output voltage when input is an AC voltage across the electrostatic combs of the driving resonator. The DC bias is +/-20 V.

When the input of the filter system is changed from a force source to a voltage source, the frequency response of the filter decreases by 1.6 kHz. This change is due to the electrical spring softening effect of the comb drives since the electrostatic forces are always attractive and therefore the combs act as springs with a negative spring constant.

Figure 10 also shows the output voltage of the interface circuit, which has the same frequency characteristic as the velocity output, but a different amplitude. In the following discussion, the filter output will refer to the output voltage of interface circuit.

4. Manufacturing Variations

In addition to the finite mass effect of beams, there are several other factors which can cause a shift of center frequency and change of bandwidth. The most common and inevitable nonideal factor is manufacturing variation.

Manufacturing variation will arise in lithography during CMOS batch fabrication, and in post-CMOS etching as well. Geometric sizes including the width of beams and comb fingers, the size of plates, and the thickness of microstructures, will all vary from the design values, so as

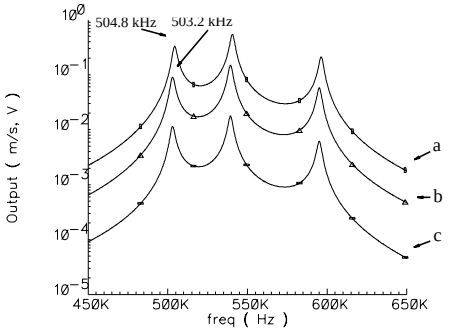

Figure 10: Different input/output variables in NODAS (a) output velocity when input is force; (b) output velocity when input is voltage; (c) output voltage of output interface circuit when input is voltage.

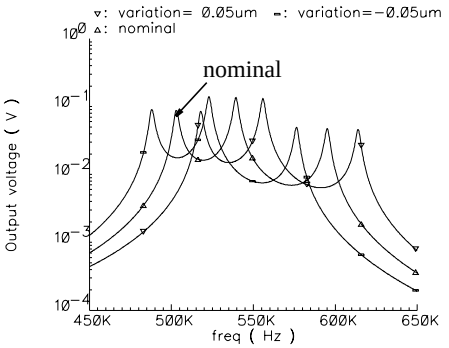

Figure 11: Simulation of Effect of manufacturing variations (correlated variation for all beams, plates and fingers)

Table 2. Simulation data for manufacturing variations

δ (μm)	f_c (kHz)	BW (kHz)
0	550	92
+0.05	566	96
-0.05	532	88

to cause variation in resonant frequency and performance of entire filter system. Assuming the variation in each dimension is correlated, Table 2 shows the center frequency and bandwidth of the nominal case and cases with a +0.05 μm and a -0.05 μm variation. Figure 11 shows the frequency response of the filter for those cases. All the beams are simulated with finite mass, for a more accurate representation of the system. The variation results in a center frequency variation ranging from 532 kHz to 566 kHz, and bandwidth ranging from 88 kHz to 96 kHz. The bandwidth is mainly determined by the stiffness of coupling springs. The softer the coupling spring, the smaller is the bandwidth.

Since the electrical spring softening effect of the comb drives affects the resonant frequency of the structure, it can be used as a frequency tuning technique to compensate manufacturing variations. Figure 12 shows that by changing the bias voltage from +/-20 V to +/-2 V, the frequency response of the case with -0.01μm variation can be corrected back by +1.4 kHz. Besides, since the comb fingers are not dedicated to tuning only, the output voltage amplitude is decreased by 40 dB with the decrease of bias voltage. To compensate bigger variation, extra tuning fingers or smaller gaps between fingers are needed.

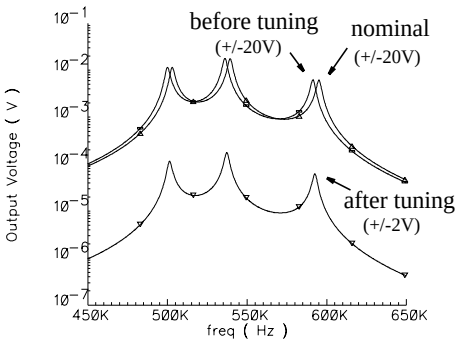

Figure 12: Effect of electrical spring softening

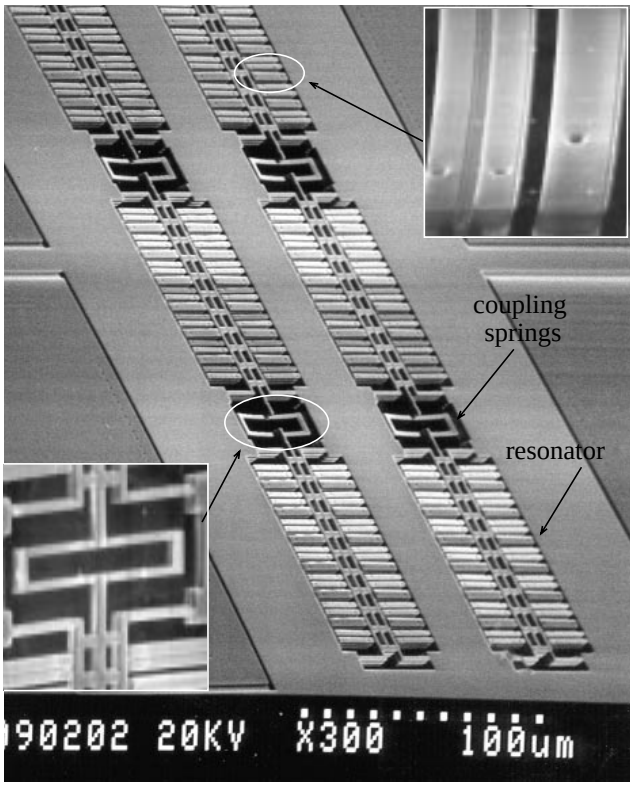

Figure 13: SEM picture and close-up pictures of two released filters.

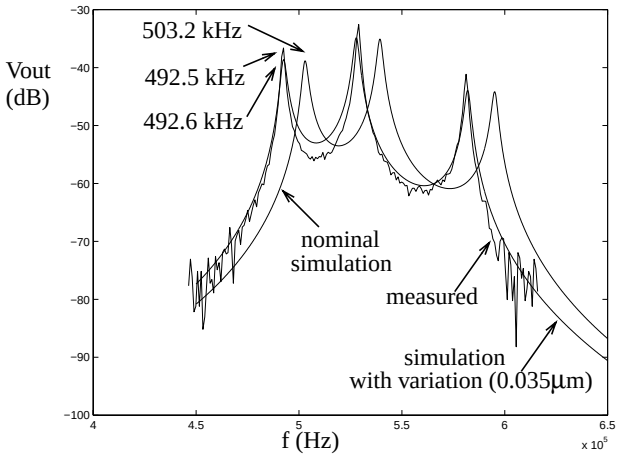

Figure 14: Measured output voltage of sensing interface circuit and output voltage from nominal NODAS simulation and simulation with a variation of 0.035 μm due to overetch.

EXPERIMENTAL RESULTS

Figure 13 shows the SEM of two released filters and the close-ups of the differential comb drive and "O" coupling spring. The device is tested in air, with bias voltage at +/-20V. Figure 14 shows the frequency response of the entire filter system (output voltage of interface circuit), with comparison to simulation. The comparison shows that NODAS nominal simulation result matches the experimental results to within 3%. And the simulation result with an variation of 0.035 μm due to overetch matches even more closely to the experimental results, which is a reasonable estimation of existing overetching.

CONCLUSIONS

A micromechanical bandpass filter, centered at 550 kHz, with a bandwidth of 92 kHz is designed, using NODAS for schematic representation and behavioral HDL simulation.

Compared to the linearized equivalent SPICE model, the NODAS methodology has advantages of easy composition and simulation iteration of complicated multi-domain systems, and of nonlinear modeling. Since NODAS models are layout-based element-level lumped parameter behavioral models, effects existing in real device elements, including finite mass of beams, electrical spring softening, and manufacturing variations are inherently modeled. Moreover, the NODAS cell library enables hierarchical simulation of systems more complicated than the bandpass filters, for which the equivalent SPICE models may be cumbersome to obtain.

Comparison of experimental results to simulation results validates NODAS models as a design tool for suspended MEMS. The designed bandpass filter is oriented to application in the IF region. However, device performance such as bandwidth and passband ripple need to be improved for practical applications, which requires further exploration of effective Q-adjustment and frequency-tuning techniques.

ACKNOWLEDGMENT

The authors would like to thank Xu Zhu for device release and taking SEMs. We also appreciate Suresh Santhanam for his help with SEMs. This research effort is sponsored by the Defense Advanced Research Projects Agency under the Air Force Research Laboratory, Air Force Material Command, USAF, under grant number F30602-96-2-0304 and in part by G.K.Fedder's National Science Foundation CAREER Award MIP-9625471.

REFERENCES

[1] K. Wang and C.T.-C. Nguyen, "High-Order Micromechanical Electronic Filters," *IEEE MEMS Workshop*, Nagoya, Japan, January 26-30, 1997, pp.25-30.

[2] C.T.-C. Nguyen, and R.T. Howe, "An Integrated CMOS Micromechanical Resonator High-Q Oscillator", *IEEE J. Solid-State Circuits*, vol. 34, No. 4, April 1999, pp.440-455.

[3] C.T.-C. Nguyen, "Frequency-Selective MEMS for Miniaturized Low-Power Communication Devices," *IEEE Trans. on Microwave Theory & Technique*, Vol. 47, No. 8, Aug. 1999, pp. 1486-1503

[4] G. K. Fedder, S. Santhanam, M.L. Reed, S.C. Eagle, D.F. Guillou, M.S. Lu, and L.R. Carley, "Laminated High-Aspect-Ratio Microstructures in a Conventional CMOS Process", *Sensors and Actuators*, v.A57, No.2, pp.103-110.

[5] G.K. Fedder and Q. Jing, "A Hierarchical Circuit-Level Design Methodology for Microelectromechanical Systems," *IEEE Trans. on Circuits & Systems II*, Vol. 46, No. 10, Oct. 1999, pp. 1309-1315.

[6] Cadence Design Systems, Inc., 555 River Oaks Parkway, San Jose, California 95134, http://www.cadence.com

[7] R.A. Johnson, Mechanical Filters in Electronics, New York: John Wiley & Sons, 1983.